

ON THE INTRINSIC INITIATION AND ARREST CLEAVAGE FRACTURE TOUGHNESS OF FERRITE– M. L. Hribernik, G. R. Odette, and M. Y. He (University of California, Santa Barbara)

OBJECTIVE

The temperature dependence of the initiation and crack arrest fracture toughness of cleavage oriented Fe single crystals have been measured. The primary objective is to assess the hypothesis that a universal master toughness temperature curve shape, $K_{Jc}(T - T_o)$, observed in structural steels, where T_o is reference temperature, derives from an underlying universal temperature dependence of the intrinsic ferrite lattice micro-arrest toughness, $K_u(T)$. These results also represent the first database on the fundamental toughness properties of Fe and will provide critical insight on the atomic processes governing the brittle-to-ductile transition (BDT).

SUMMARY

The results of the crack arrest fracture toughness (K_a) measurements on cleavage oriented Fe single crystals from -196 to 0°C are reported. The corresponding static (K_{Ic}) and dynamic (K_{Id}) cleavage initiation toughness between -196 to 25°C were also measured over a range of applied stress intensity rates (K_I') from ≈ 0.1 to $>10^4$ MPa $\sqrt{m/s}$. The $K_{Ia}(T)$, $K_{Ic}(T)$, and $K_{Id}(T)$ gradually increase with temperature (T) from a minimum average K_{Ia} value of about 3.85 ± 1.3 MPa \sqrt{m} up to a rapid BDT at $\approx 0^\circ\text{C}$. The minimum average K_{Ia} is roughly twice the theoretical estimate of the brittle fracture Griffith toughness. The BDT temperature increases with higher K_I' and is highest for K_{Ia} . The K_I' dependence of $K_{Ic/d}(T)$ is consistent with the strain rate dependence of thermally activated flow stress of Fe. The $K_{Ic}(T)$ for single crystal Fe and W (Gumbsh) are also reasonably similar when plotted on a homologous temperature scale. The $K_{Ia}(T)$ for Fe at $\approx -30^\circ\text{C}$ is similar to that for 3%Si-Fe (Argon) at $\approx 110^\circ\text{C}$. This $\approx 140^\circ\text{C}$ shift can be reasonably rationalized by the solid solution lattice strengthening of Si. The $K_{Ia}(T)$ for Fe must be shifted up by $\approx 225^\circ\text{C}$ to approximate the temperature dependence of the $K_u(T)$ that is consistent with a universal $K_{Jc}(T)$ master curve shape. This magnitude of shift may be caused by a combination of thermally activated (rate-dependent) solid solution lattice strengthening, complemented by long-range internal stress fields.

PROGRESS AND STATUS

Introduction

The brittle-to-ductile transition (BDT) in bcc metals and alloys is of both technological and scientific importance. Almost no reliable experimental data have been available on the BDT in Fe, and, in spite of a large modeling literature, a fundamental understanding of the BDT remains one of the most elusive 'grand challenges' of materials science. A corollary fundamental challenge is to rationalize the empirical observation that the shape of the macroscopic fracture toughness-temperature curve, $K_{Jc}(T - T_o)$, of structural steels is the approximately same when scaled by reference temperature T_o . The universal master curve (MC) shape appears to apply to a very wide range of alloy microstructures and strength levels, thus a correspondingly large span of T_o . The ASTM Standard E 1921 [1] for measuring fracture toughness in the transition is based on the MC concept. However, there are a number of questions concerning the MC method. The most fundamental pertains to the existence of a universal MC shape, which is not understood [2].

Cleavage in steels involves a sequence of events ultimately associated with the unstable propagation of a microcrack formed at brittle trigger particle. Under small scale yielding conditions, self-similar stress and strain field concentrations develop in the vicinity of a loaded blunting crack. The peak tensile stresses, σ_{22} , reach levels of 3 to 5 times the yield stress, σ_y . The area A within a specified σ_{22}/σ_y contour increase in proportion to $K_J^4/[E/(1-\nu^2)]^2$, where K_J is the elastic-plastic crack loading parameter, E is the elastic modulus and ν is Poisson's ratio. The high stresses and strains in the blunting crack tip process zone crack brittle trigger particles, like grain boundary carbides and inclusions (or clusters of such features). While many particles may break in the process zone, only those with sufficiently large size and favorable

orientation with respect to low cleavage toughness crystallographic planes and directions in the adjoining ferrite are 'eligible' for a microcrack propagation event. That is, the propagation, versus arrest, of a dynamic microcrack into the adjacent ferrite matrix is the critical event for macroscopic cleavage [3,4]. Because of the distribution of the largest and properly oriented particles in any sampling volume, cleavage is basically a statistical process, leading to a wide specimen-to-specimen distribution of the measured fracture toughness. However, the mean (or median) cleavage condition be described in terms of a critical stress contour $\sigma_{22} = \sigma^*$ encompassing a critical volume V^* of material in the process zone, $V^* = A^*B$, where A^* is a critically stressed in-plane area and B is the specimen thickness [2,3]. The critical σ^*-A^* constitutes the local cleavage fracture property that depends on the trigger particle microstructure, and the corresponding K_{Jc} depends on the σ^*-A^* and the constitutive properties, $\sigma(\varepsilon)$, of the steel. The loading increases until cleavage occurs $K_J = K_{Jc}$ at $\sigma_{22} = \sigma^*$ and $A(\sigma_{22}) = A^*$ [2-3].

The σ^* can be expressed in terms of a modified Griffith criteria in Equation 1 [2-4]:

$$\sigma^* = CK_{\mu}/\sqrt{d} \quad (1)$$

Here, C is a geometric factor, of order unity, that depends on the assumed trigger particle crack shape and d is the characteristic trigger particle size. Thus the macroscopic cleavage K_{Jc} is controlled, or valued, by the K_{μ} ($\ll K_{Jc}$) of ferrite.

Finite element simulations of crack tip fields for a specified $\sigma(\varepsilon)$ can be used to evaluate the fields, hence, K_{Jc} at $\sigma_{22} = \sigma^*$ and $A(\sigma_{22}) = A^*$ [2,3,5]. The temperature-dependence of $K_{Jc}(T)$ is mediated by the temperature dependence of $\sigma(T,\varepsilon)$ and $\sigma^*(T)$, since A^* primarily depends only on the microstructure. At low temperatures the σ^*-A^* $K_{Jc}(T)$ model predictions are consistent with the MC shape based on the traditional assumption that σ^* is approximately independent of temperature. In this case, the temperature dependence of $K_{Jc}(T)$ is fully controlled by the corresponding thermally activated component of $\sigma_y(T)$, which is similar in most Fe based bcc alloys.

Irradiation of ferritic steels produces nano-scale precipitates and defect clusters that result in a temperature independent increase in the athermal yield and flow strength, and a corresponding upward shift in T_0 . The coarser scale microstructure is unaffected. As T_0 increases, due to a $\Delta\sigma_y$, the constant σ^*-A^* model predicts a reduction (layover) of the MC slope in the transition that are not observed experimentally [1-3]. These layovers are a consequence of the decreasing temperature dependence of $\sigma_y(T)$ at higher $T_0 \geq \approx 0^\circ\text{C}$. The inconsistency between model and observation can be remedied by incorporating a modest temperature dependence in $\sigma^*(T)$.

The temperature dependence of $\sigma^*(T)$ demands a corresponding temperature dependence of $K_{\mu}(T)$. The fact that the position (T_0), but not the shape, of the MC depends on microstructure and alloy strength leads to the hypothesis that $K_{\mu}(T)$ is independent of the fine, nano-scale features such as those introduced by irradiation. This further suggests that some intrinsic property of the ferrite matrix controls $K_{\mu}(T)$. Thus the focus of this work is on assessing $K_{\mu}(T)$ in Fe. While it can be inferred from the trigger particle size distribution and σ^* , K_{μ} cannot be directly measured [2-4]. However, it is possible to measure various toughness parameters of single crystal Fe single crystals oriented for cleavage, including the static (K_{Ic}) and dynamic (K_{Id}) initiation toughness for sharp cracks, as well as the arrest toughness (K_{Ia}) for propagating cracks. While certainly not identical properties, we propose that the $K_a(T)$ is a good surrogate for $K_{\mu}(T)$. Indeed, K_{Ic} , K_{Id} , K_{Ia} , and K_{μ} all reflect the fundamental phenomena of the BDT in Fe.

In spite of the paucity of data, many models have been proposed to describe the BDT in Fe and other bcc metals and alloys. Regardless of detail and level of approximation, however, most BDT models are based on the interaction between a (usually) sharp crack tip under increasing remote loading (K_I) and the evolution of local dislocation structures, that alters (shields) the elastic crack tip field and dissipates energy. The shielding reduces the effective crack tip stress intensity factor k_t relative to the K_I , $k_t/K_I < 1$. As K_I and k_t increase, the local stresses may, or may not, reach a level capable of breaking bonds; or

from an energy balance perspective, k_t may ($T < T_{BDT}$) or may not ($T > T_{BDT}$) reach the brittle fracture Griffith criteria k_g . The first successful attempt to model the BDT, based on an energy criterion mediating the nucleation of a single dislocation (ductile) prior to bond breaking (brittle), was proposed by Rice and Thomson (RT) [6]. The RT model and its progeny focusing on the nucleation and glide of dislocations, coupled with some detailed experimental observations, have helped to clarify the specific crystallographic slip processes involved in shielding a stationary crack tip. However, the various BDT models involve a number of assumptions and approximations and predict a wide range of behavior. Indeed, the models and model parameters, such as the type and spacing of dislocation sources [7], can be adjusted to match wide range of experimental results [frequently based on inappropriate choices like the macroscopic $K_{Jc}(T)$]. Further, the BDT models have generally not addressed the crack tip processes involved in continued propagation of a cleavage crack, or arrest of the crack by the evolution of crack tip shielding dislocations. Thus, it is clear that the atomic level processes that govern the BDT are not fully understood in general, and for crack arrest in particular. Hence, our major objective is to develop a unique database of initiation and arrest toughness of unalloyed Fe single crystals over a wide range of temperature.

Experimental Procedures

The following section only very briefly outlines the challenging experimental techniques used in this study. Additional details will be provided in future reports. Single crystal rods slightly less than 1 cm in diameter and 5–6 cm in length with orientations consistent with EDM sectioning into thin rectangular slices with the desired (100)[010] and (100)[011] cleavage plane and crack direction orientations were procured from Monocrystals Corporation. The crystal orientations were confirmed by Laue back reflection x-ray diffraction. The most significant challenge was to design a specimen and test procedure that allowed the initiation and arrest of a cleavage crack in the very small distance (< 8 mm) that was available. As illustrated in Fig. 1, properly oriented single crystal slices were incorporated into composite specimens reflecting two different approaches to testing. Both types of composite specimens were fabricated by diffusion bonding, and in some cases brazing, the single crystal slices to high strength steel sections that served both to transmit loads and store and release elastic energy.

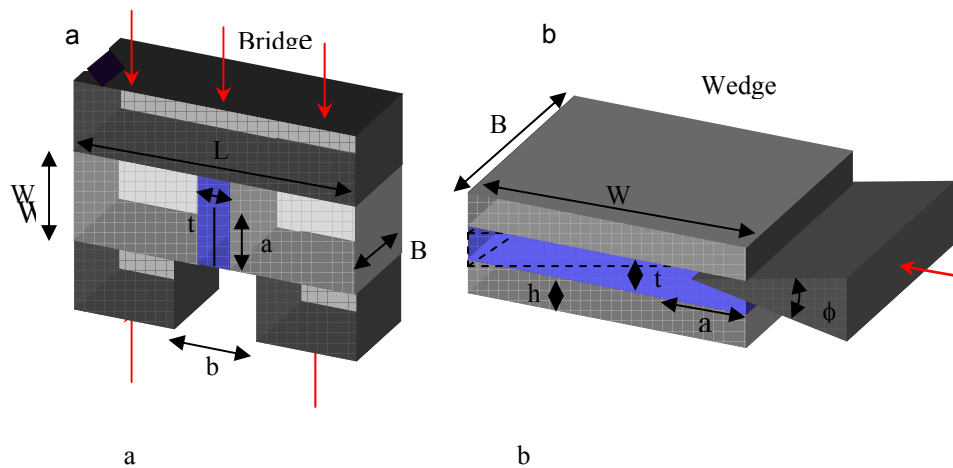


Fig. 1. The a) bridge anvil specimen and b) double cantilevered beam chevron wedge specimen.

The first technique was a modified compression anvil bridge method shown in Fig. 1a. The beam initially contains a shallow fatigue pre-crack. When loaded with a compressive stress (σ) parallel to the propagation direction, Poisson stresses act normal to the crack faces and elastic energy is released as the crack propagates. The blue lines in Fig. 2a show the variation in the corresponding normalized stress intensity factor ($K_I/\sigma W^{1/2}$) versus the crack depth to beam width ratio (a/W) determined from detailed finite element (FE) analysis. The FE analysis was used to quantify and optimize the compression anvil bridge method (which had been used previously for pre-cracking ceramics [8]), considering many geometric factors and other details, such as the effect of the different modulus in the single crystal versus the steel beam arms (the dashed versus the solid curve). The $K_I/\sigma W^{1/2}$ for the compression anvil bridge method first increases from the shallow starting crack depth to a maximum at $a/W \approx 0.2$ and then decreases rapidly with increasing a/W , resulting in crack arrest. Thus the K_{Ia} is simply determined from the final a/W and the σ at initiation (note there is no load drop as the crack propagates). The major limitation of the compression anvil bridge technique is that at higher test temperatures ($T > -100^\circ\text{C}$) it is not possible to initiate a dynamic crack from a shallow fatigue pre-crack at a compressive σ that does not damage or deform the specimen.

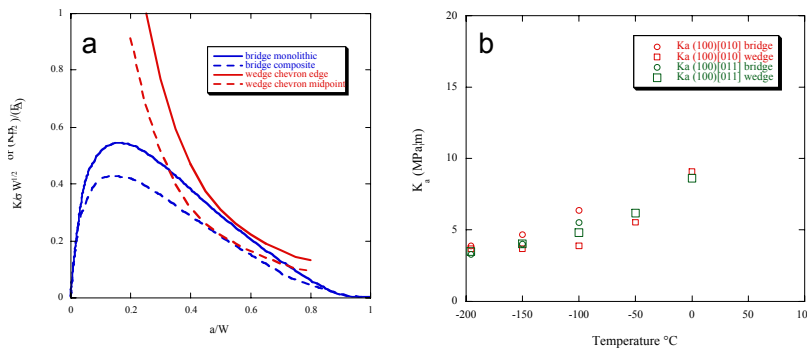


Fig. 2. The a) normalized stress intensity curves as a function of crack length for initiation and arrest events in the bridge and double cantilevered beam chevron wedge specimens and b) K_{Ia} as a function of temperature measured by the boyh techniques from ≈ -196 to 0°C for both Fe single crystal orientations.

Thus a second method was developed based on the wedge loading of a composite chevron specimen with short double cantilever arms as shown in Fig. 1b. This test is a modification of the so-called short beam test [9]. The composite double cantilever beam chevron technique allowed access to higher test temperatures up to $\approx 0^\circ\text{C}$ and has the advantage that multiple initiation and arrest events can be measured with a single specimen. Implementation of this test method also required a FE detailed analysis and optimization, leading to the normalized stress intensity factor ($K_{Ib}^{1/2}/E\Delta$) shown by the red lines in Fig. 2a, where Δ is the wedge opening displacement at the end of the beam arms. The $K_{Ib}^{1/2}/E\Delta$ decreases continuously with a/W in this case. Thus, this test is carried out by slowly inserting the wedge into mating surfaces on the beams, stopping immediately when the crack propagates and arrests at a critical Δ_c , measured by a clip gauge attached to the end of the beams. The K_{Ic} and K_{Ia} are determined from the measured Δ_c and the initial and final a/W , respectively. The a/W are determined from benchmark lines on the fracture surface. One very important detail about the double cantilever beam chevron wedge test determined in the FE analysis was that the K_I is significantly higher at the edge corners (solid line) of the crack front in the chevron than is the center (dashed line). Thus, cracks tend to initiate at the corners (at K_{Ic}) and arrest (at K_{Ia}) in the middle of the crack front. Thus it is necessary to use the appropriate calibration curve in each case. Crack 'pop-ins' were detected using acoustic emission monitors for both types of tests, augmented by crack gauges for the compression anvil bridge technique. Both techniques were 'calibrated' using TiAl with an initiation K_{Ic} of $\approx 7.1 \pm 0.5 \text{ MPa}\sqrt{\text{m}}$ and a $K_{Ia} \approx 3.2 \pm 0.7 \text{ MPa}\sqrt{\text{m}}$.

